GENERALIZED ANALYTICAL DESIGN OF BROADBAND PLANAR BALUNS BASED ON WIRE-BONDED MULTICONDUCTOR TRANSMISSION LINES

Juan-José Sánchez-Martínez[*] **and Enrique Márquez-Segura**

Departamento de Ingeniería de Comunicaciones, Escuela Técnica Superior de Ingeniería de Telecomunicación, Campus de Teatinos, Málaga 29071, Spain

Abstract—A novel generalized design procedure of broadband planar baluns based on wire-bonded multiconductor transmission lines (MTL) is presented hereby based on analytical equations. The proposed balun consists of two parts. The first one is an in-phase power divider, which equally splits the input power through its two outputs. The later are two MTLs with wire bonding between alternate conductors configured to introduce +90 and −90 degrees phase shift respectively, so that the balanced output signal has a 180 degree phase difference. In that sense, new closed-form design equations in order to calculate the design parameters of both multiconductor elements are obtained. These equations allow the proper dimensions of both MTLs to be computed irrespective of both the number of conductors and the coupling factor, and therefore, to determine the performance of the balun. The design procedure for wire-bonded MTL baluns has been assessed by means of full-wave electromagnetic simulations and by experimental work. In addition, the very good agreement between the theoretical results and measurements makes possible to define a time-saving design methodology.

1. INTRODUCTION

Baluns are important 3-port devices necessary for feeding differential devices such as two-wire antennas, balanced mixers, push-pull amplifiers, balanced modulators, and many other applications. The primary function of a balun is to convert an unbalanced input signal into a balanced differential output one.

Different baluns configurations have been reported by using sections of single or coupled transmission lines. Planar baluns based on coupled lines can be divided into two groups, quarter-wave coupled line baluns and Marchand coupled-line baluns [1]. Examples of the first group can be found in [2–4] while for the second group there is an extensive quantity of publications [5–9].

In this work, a planar balun configuration consisting of two sections is considered (Fig. 1). The first section is a power divider which provides two well-balanced equal amplitude in-phase signals over a broad frequency range. The second section provides −90 degrees and +90 degrees phase shift over these two signals, so the balanced output signals have a 180 degree phase difference [10–14]. A Wilkinson in-phase power divider has been usually employed for the power splitter due to its broadband operation and good input/output match and isolation. The last condition improves the main Marchand balun drawback, its poor balanced output ports matching and isolation [15]. For the phase shifter section, short-circuited and open-circuited coupled lines have been employed in [10, 11] but, there is lack of both a design procedure and analysis for wire-bonded multiconductor transmission lines (MTL). The presented balun circumvents the limited output isolation and narrow operating bandwidth of most of the recently published baluns. Consequently, the use of wire-bonded MTLs is advisable in designing wideband baluns because both short- and open-circuited MTLs are dual components, and if they are properly designed a perfect theoretical output amplitude and phase balance can be achieved at all frequencies. By using this type of balun, a reconfigurable test-set that allows the measurement of both, differential and common modes S-parameters using a commercial two-port vector network analyzer was presented in [16], where the isolation between output ports is critical.

Therefore, in this paper a design guideline is given when multiconductor transmission lines with bonding wires between alternate conductors are used as a 180° phase shifter (Fig. 1). This MTL is a specific case of multiconductor transmission lines [1, 17, 18] in which bonding wires interconnect the ends of alternate conductors. This particular configuration (wire-bonded MTL) improves the operating bandwidth by eliminating undesired resonances and allows circuit designers to use simplified analytical models [19]. Assuming ideal short circuits across alternate conductors (bonding wires very short compared to wavelength), the connections can be neglected and the equivalent model of a wire-bonded MTL can be simplified as a pair of coupled lines [1, 20]. Results presented herein are particularly helpful in designing baluns using closed-form design equations irrespective of

the number of conductors and the coupling factor and new equations are advisable for designing devices based on coupled lines where it is necessary to control both the magnitude and the phase of the frequency response. Accordingly, it is important to remark that this theory can be also employed to design coupled-line ring hybrids [21], artificial composite right/left handed transmission lines [22, 23], rat-race couplers [24], filters [25, 26], impedance transformers [27], power dividers [28], and so on. Further, in keeping with the trend toward miniaturization, the comprehensive analysis of the wire-bonded MTL is essential, even more with the recent upsurge in systems based on coupled lines [24–28].

2. ANALYSIS AND DESIGN OF THE WIRE-BONDED MTL BALUN

2.1. Balun Architecture

The circuit schematic of the proposed planar balun, consisting of a power divider connected to two wire-bonded multiconductor transmission lines, is sketched in Fig. 1. The power divider splits the input signal into two equal amplitude in-phase signals. Then, the two output signals pass through a pair of short-circuited and open-circuited MTLs configured to introduce +90 and −90 degrees phase shift respectively, over each signal. Therefore, output signals have equal amplitude and 180 degrees phase difference. According to the power divider, the Wilkinson divider seems to be a good choice because
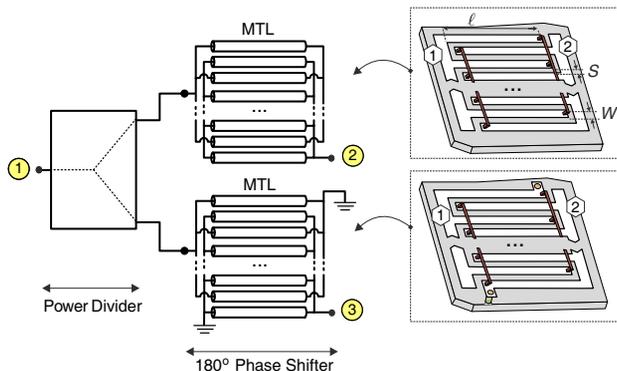
Figure 1. Architecture of the balun consisting of an in-phase power divider and two wire-bonded multiconductor transmission lines. A snapshot of a wire-bonded MTL in microstrip technology is included.

it provides equal power split, high output ports isolation and good match at all three ports. Besides, the Wilkinson can be designed with multiple stages in order to enlarge its bandwidth and fulfill the frequency band requirements.

2.2. Theoretical Study of Open- and Short-circuited Wire-bonded MTLs

A wire-bonded multiconductor transmission line is a four-port device and its input admittance matrix can be found in [29]. By placing open or short-circuits at its diagonal ports, the two-port circuits drawn in the insets of Fig. 1 are obtained. When losses are neglected and coupling between non adjacent strips is negligible, both devices are characterized by the following admittance matrices

$$[Y]_o = \frac{(M^2 - N^2)\sin\theta}{M^2\cos^2\theta - N^2}\begin{bmatrix} jM\cos\theta & jN \\ jN & jM\cos\theta \end{bmatrix} \tag{1}$$

$$[Y]_s = \frac{1}{\sin\theta}\begin{bmatrix} -jM\cos\theta & jN \\ jN & -jM\cos\theta \end{bmatrix}, \tag{2}$$

where the subscripts o and s stand for the open-circuit or short-circuit boundary conditions respectively. θ is the electrical length of the conductors, and M and N are defined by

$$M = \frac{(k-1)\left(Y_{oe}^2 + Y_{oo}^2\right) + 2Y_{oe}Y_{oo}}{2\left(Y_{oe} + Y_{oo}\right)}, \quad N = \frac{(k-1)\left(Y_{oe} - Y_{oo}\right)}{2}. \tag{3}$$

where Y_{oo} and Y_{oe} are the odd and even modes admittances respectively, of a pair of adjacent lines and k relates to the number of strips. When no losses are considered Y_{oo} and Y_{oe} are real numbers and $M > 0$, $N < 0$ and $M^2 > N^2$ [29]. It is important to remark that in previous equations it has been considered that both wire-bonded MTLs are equal and only the boundary conditions, short-circuit or open-circuit, are changed. Besides, pure TEM and lossless propagation are assumed, θ being the average value of the even- and odd-mode electrical lengths. This approximation allows us to obtain a simplified analytical model of the wire-bonded MTL in an inhomogeneous dielectric. The validity and accuracy of this approximation has been investigated and validated in [1, 20, 30, 31], where it was demonstrated an excellent agreement between experimental results and the values obtained by using the average value of the even- and odd-mode electrical lengths.

The propagation constant of the two-port structures obtained can be calculated from (1) and (2) as [32]

$$\cosh(\gamma\ell) = \frac{(Y_{11}Y_{22})^{1/2}}{Y_{21}}, \tag{4}$$

ℓ being the length of the MTL. When both wire-bonded MTLs are assumed lossless (4) is simply given by

$$\beta_o \ell = \cos^{-1}\left(-\frac{M}{N}\cos\theta\right), \quad \beta_s \ell = \cos^{-1}\left(\frac{M}{N}\cos\theta\right) \tag{5}$$

where clearly it is observed that $\beta_s = \beta_o + \pi$. Thus, the output signals of the open- and short-circuited MTLs are always 180 degree out-of-phase at all frequencies. Nevertheless, such equations are deduced considering that input and output ports are perfectly matched. The image impedances of both circuits can be calculated from (1) and (2) as

$$Z_{I_o} = \frac{\left(N^2 - M^2\cos^2\theta\right)^{1/2}}{(M^2 - N^2)\sin\theta}, \quad Z_{I_s} = \frac{\sin\theta}{\left(N^2 - M^2\cos^2\theta\right)^{1/2}} \tag{6}$$

As seen, both image impedances are different and depend on the electrical length of the MTL. Consequently, it is necessary to find out some design rule in order to obtain 180 degrees differential phase and equal amplitude outputs. By means of simple transformations [32] and after some algebraic manipulations, the reflection S_{11} and transmission S_{21} coefficients of each wire-bonded MTL (see the insets in Fig. 1) are given by

$$S_{11_i} = \frac{K_i^2(N^2 - M^2\cos^2\theta) - Z_0^2}{\Delta_i} \tag{7a}$$

$$S_{21_i} = \frac{2G_i K_i Z_0 N}{j\Delta_i}, \tag{7b}$$

where Z_0 is the reference impedance, and the subindex i can be o or s depending on whether the S-parameters of the open-circuited MTL or short-circuited MTL are evaluated. The variables Δ_i, K_i and G_i are defined as

$$\Delta_i = K_i^2\left(N^2 - M^2\cos^2\theta\right) + Z_0^2 + j2K_i Z_0 M\cos\theta \tag{8a}$$

$$K_o = \frac{1}{(N^2 - M^2)\sin\theta}; \quad G_o = +1 \tag{8b}$$

$$K_s = \frac{\sin\theta}{M^2\cos^2\theta - N^2}; \quad G_s = -1. \tag{8c}$$

These expressions are useful because valuable information as frequency response, operating bandwidth, phase balance, etc. can be easily calculated. If the condition

$$|S_{21_o}|e^{j\phi} = |S_{21_s}|e^{j(\phi+\pi)} \tag{9}$$

is imposed on (7b), the next equality is obtained

$$Y_0^2 = M^2 - N^2 = Y_{oe}Y_{oo} \frac{([[(k-1)+u][(1+u(k-1)]]}{(1+u)^2}, \qquad (10)$$

which determines a specific relation between the even and odd mode impedances, being $u = Z_{oe}/Z_{oo}$. Therefore, whenever Equation (10) is fulfilled, the output signals have equal amplitude and a phase difference of 180 degrees. Nevertheless, although output signals have equal amplitude, it does not imply to have a good impedance matching. Consequently, another condition related to port matching is necessary. Substituting (10) in (7a), it is found that

$$\cos^2 \theta_d = 2 - \frac{M^2}{N^2} = 2 - \left(\frac{2u + (k-1)(1+u^2)}{(k-1)(1-u^2)} \right)^2, \qquad (11)$$

where θ_d stands for the electrical length at which the MTL is match-terminated ($S_{11} = 0$). Accordingly, there are two design equations: by using (10) a good amplitude and phase balance is guaranteed, and by means of (11) it is straightforward to control the point of perfect match of both short- and open-circuited MTLs. This implies that the image impedance of both structures is equal to the reference impedance Z_0 at θ_d. Equation (11) can be expressed as

$$u = \frac{Z_{oe}}{Z_{oo}} = \frac{1 + \sqrt{(1+(k-1)^2 \sin^2 \theta_d)}}{(k-1)\left(\sqrt{1+\sin^2 \theta_d} - 1 \right)}, \qquad (12)$$

that, given the number of strips k, allows the values of u to get a perfect input match at θ_d to be computed. The values of u are shown
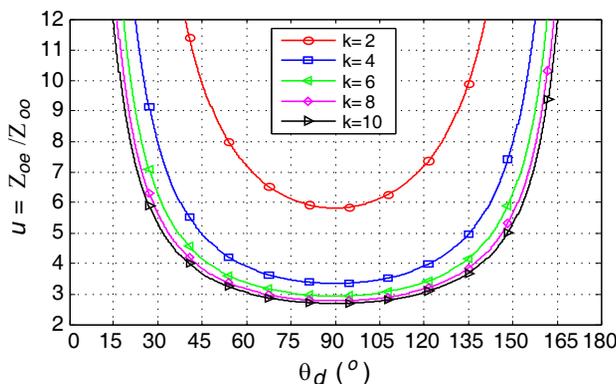
Figure 2. $u = Z_{oe}/Z_{oo}$ as a function of θ_d for several number of conductors k according to (12).

in Fig. 2 as a function of both, θ_d and the number of conductors of the MTL. As seen, only for $\theta_d = 90°$ the value of u is unique, and for another higher Z_{oe}/Z_{oo} ratio, the MTL will have two ideal input match frequencies within the operating frequency band. In addition, the greater the number of conductors the lower Z_{oe}/Z_{oo} ratio for each θ_d, that is directly related to more feasible physical dimensions (width and spacing between strips). Furthermore, it is also noticeable how the reduction by passing from $k = 2$ to $k = 4$ or $k = 6$ is significative, but using a higher number of conductors can be counter-productive because the reduction in u is small compared to the manufacturing complexity that it involves.

Consequently, once the $u = Z_{oe}/Z_{oo}$ ratio has been chosen taking into account (12), Equation (10) can be split as

$$\frac{Z_{oe}}{Z_0} = \frac{\sqrt{u[(k-1)+u][1+u(k-1)]}}{(1+u)} \tag{13a}$$

$$\frac{Z_{oo}}{Z_0} = \frac{\sqrt{[(k-1)+u][1+u(k-1)]}}{\sqrt{u}(1+u)}, \tag{13b}$$

in order to compute the proper values of the even- and odd-mode impedances that guarantee an ideal output amplitude and phase balance at all frequencies, and a perfect input match at one ($\theta_d = 90°$) or two single frequencies ($\theta_d \neq 90°$).

If the aforementioned design procedure is followed, some expressions can be simplified. Firstly, M and N can be rewritten as

$$\frac{M^2}{Y_0^2} = \frac{1 + \sin^2 \theta_d}{\sin^2 \theta_d}, \quad \frac{N^2}{Y_0^2} = \frac{1}{\sin^2 \theta_d}, \tag{14}$$

where $Y_0 = 1/Z_0$. From (14), the most remarkable property is that neither M nor N no longer depend on the number of conductors and are determined by only a function of θ_d. Therefore, regardless of the number of conductors, if the even and odd mode impedances Z_{oe} and Z_{oo} are selected according to (12) and (13), all previous equations are drastically simplified. Hence, expressions for the image impedances (6) are reduced to

$$\frac{Z_{I_o}}{Z_0} = \left(1 + \frac{\sin^2 \theta - \sin^2 \theta_d}{\sin^2 \theta \, \sin^2 \theta_d}\right)^{1/2}, \quad \frac{Z_{I_s}}{Z_0} = \left(1 + \frac{\sin^2 \theta - \sin^2 \theta_d}{\sin^2 \theta \, \sin^2 \theta_d}\right)^{-1/2}. \tag{15}$$

Figure 3 represents the real part of both normalized impedances as a function of θ for several values of θ_d. As seen, only for $\theta = \theta_d$ curves are equal to unity and thus, the impedance matching is perfect. Besides, two singularities are observed, θ_1 and θ_2, which are the poles of both functions in (15) and determine the frequency range where
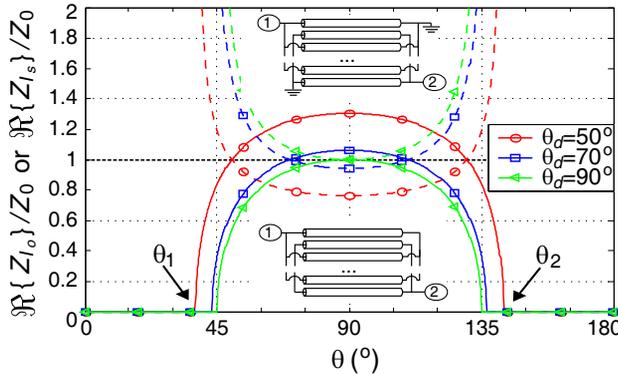
Figure 3. Real part of normalized image impedances for two short- and open-circuited MTL designed by means of (12) and (13) as a function of θ for several number of θ_d (frequencies of ideal match).

the image impedances pass from being purely real impedances to purely imaginary, capacitive and inductive reactances for the short-circuited and open-circuited elements, respectively. These singularities are calculated as

$$\theta_1 = \arccos\left(\frac{|N|}{M}\right) = \arccos\left(\frac{1}{\sqrt{1 + \sin^2 \theta_d}}\right), \quad \theta_2 = 180° - \theta_1. \quad (16)$$

For the particular case $\theta_d = 90°$, $\theta_1 = 45°$ and thus, the frequency band of real impedances ranges from $\theta_1 = 45°$ up to $\theta_2 = 135°$. From (14), equations for S-parameters, (7a) and (7b), can be also simplified as

$$S_{11_o} = \frac{\sin^2 \theta - \sin^2 \theta_d}{P - jQ} \quad S_{11_s} = \frac{-\sin^2 \theta + \sin^2 \theta_d}{P - jQ} \quad (17a)$$

$$S_{21_o} = \frac{2\sin\theta \, \sin\theta_d}{Q + jP} \quad S_{21_s} = \frac{-2\sin\theta \, \sin\theta_d}{Q + jP}, \quad (17b)$$

with

$$P = \sin^2 \theta + \sin^2 \theta_d \left(1 - 2\cos^2 \theta\right) \quad (18a)$$

$$Q = \sin(2\theta) \sin\theta_d \sqrt{1 + \sin^2 \theta_d}. \quad (18b)$$

By analyzing (17a) and (17b), it is easy to observe that S_{11} and S_{21} parameters have equal magnitude but a phase difference of 180 degrees for the short- and open-circuited MTL. Moreover, a new simplification

can be obtained to compute the magnitude of such parameters as

$$|S_{11_o}| = |S_{11_s}| = \frac{|\sin^2\theta - \sin^2\theta_d|}{\sin^2\theta + \sin^2\theta_d} \tag{19a}$$

$$|S_{21_o}| = |S_{21_s}| = 2\frac{|\sin\theta \ \sin\theta_d|}{\sin^2\theta + \sin^2\theta_d}, \tag{19b}$$

which, compared to (7a) and (7b), are valuable equations by their simplicity. These expressions will be used in next sections to evaluate the performance of both MTLs.

2.3. Bandwidth Considerations

In this point, the design procedure described in Section 2.2 is evaluated. Firstly, the $u = Z_{oe}/Z_{oo}$ values to achieve perfect match at several θ_d are computed by means of (12). Then, using (13) the even and odd mode normalized impedances are obtained. Table 1 collects all these values for several number of strips, which can be directly translated to physical dimensions making previously a de-normalization operation by Z_0.

By using the values given in Table 1, Fig. 4(a) and Fig. 4(b) draw the S_{11} (19a) and S_{21} (19b) parameters. As expected, perfect match and thus, the minimum of S_{11}, is located at θ_d and, only for $\theta_d = 90°$ the S_{21} presents a maximally flat response. For any other value of θ_d a rippled response is obtained. In addition, to verify that both parameters are equal in magnitude but with 180 degrees out-of-phase

Table 1. Normalized Z_{oe} and Z_{oo} to get balanced equal amplitude out-of-phase output signals and perfect match at θ_d.

$\frac{Z_{oe}}{Z_0}, \frac{Z_{oo}}{Z_0}$	k=2	k=4	k=6	k=8	k=10
$\theta_d=50°$	2.95	4.02	5.40	6.84	8.30
	0.34	0.89	1.41	1.93	2.44
$\theta_d=60°$	2.68	3.78	5.14	6.55	7.98
	0.37	0.97	1.52	2.07	2.62
$\theta_d=70°$	2.52	3.63	4.98	6.37	7.78
	0.40	1.01	1.60	2.17	2.74
$\theta_d=80°$	2.44	3.55	4.89	6.27	7.67
	0.41	1.04	1.64	2.22	2.81
$\theta_d=90°$	2.41	3.52	4.86	6.24	7.64
	0.41	1.05	1.65	2.24	2.83
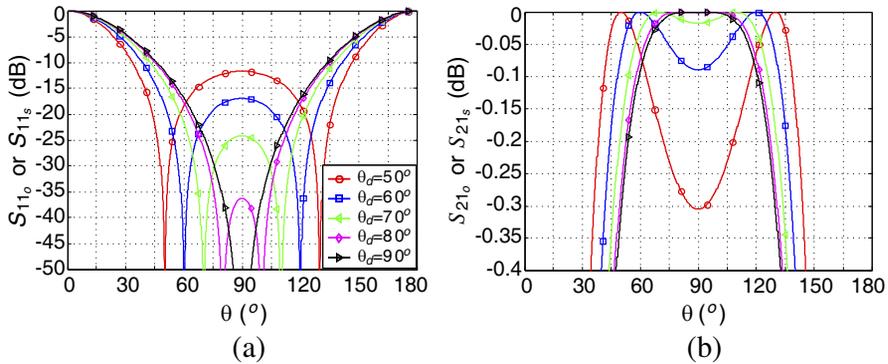
Figure 4. (a) S_{11} and (b) S_{21} of two short- and open-circuited MTL designed using values of Table 1 as a function of θ for several θ_d.
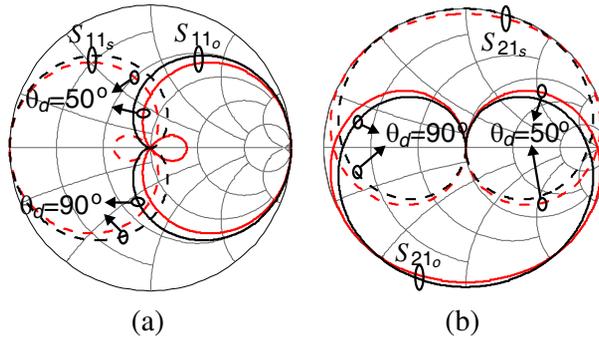

Figure 5. (a) S_{11} and (b) S_{21} of two short- and open-circuited MTL designed using values of Table 1 as a function of θ for $\theta_d = [50°, 90°]$.

for the short- and open-circuited wire-bonded MTL, Fig. 5 draws S_{11} and S_{21} on a Smith chart for two values of θ_d, $50°$ and $90°$.

The magnitude of the ripple of S_{21} can be calculated at $\theta = 90°$ in (19b), or equivalently, from (19a) it is possible to determine the magnitude of S_{11} at $\theta = 90°$ and thus, to set a return loss limit. Considering $S_{21_{lim}} = \sqrt{0.9}\,(S_{11_{lim}} = -10\,\text{dB})$ as the conventional threshold limit value at the center frequency ($\theta = 90°$), it is easy to obtain that $\theta_{d_{lim}} = 46.1°$ is the limit value that could be used. This value can be computed as

$$\theta_{d_{lim}} = \arcsin\left(\frac{1 - \sqrt{1 - S_{21_{lim}}^2}}{S_{21_{lim}}}\right). \qquad (20)$$
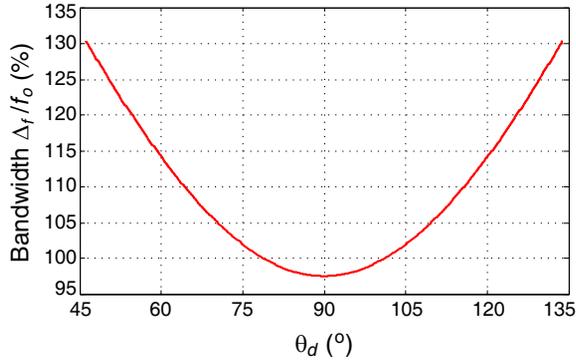
Figure 6. Fractional bandwidth for two open- and short-circuited MTLs designed by means of (12) and (13) as a function of θ_d that guarantees $S_{21} > -0.9\,\text{dB}$, $S_{11} < -10\,\text{dB}$, and a phase difference of $180°$ at their outputs.

Fig. 6 depicts the operating bandwidth as a function of θ_d, of a pair of short- and open-circuited wire-bonded MTLs that guarantees insertion loss lower than $0.9\,\text{dB}$, return loss higher than $10\,\text{dB}$ and a perfect amplitude and phase balance at all frequencies. As seen in Fig. 6, the minimum bandwidth is achieved at $\theta_d = 90°$ and it broadens as θ_d separates from such value. Consequently, in order to broaden the operating bandwidth, both MTLs should be designed to have two ideal input match frequencies ($\theta_d \neq 90°$). However, as was shown in Fig. 2, this involves using higher values of $u = Z_{oe}/Z_{oo}$, that directly implies to increase the coupling level. As a result, there is a trade-off between the operating frequency band of both MTLs and the required coupling level.

3. EXPERIMENTAL VALIDATION

In this section, in order to demonstrate the proposed design methodology, a balun is fabricated and measured. Firstly, the $180°$ phase shifting section is analyzed, and after that, it is connected to a power divider to build the whole system. The divider is a three-section Wilkinson power divider designed to provide equal power split between the two outputs [33]. The use of a multi-stage Wilkinson power divider is necessary to guarantee a bandwidth larger than the one of the MTL structures, but thanks to this, it is possible to obtain an excellent output isolation. Consequently, depending on the application, this property may be more important than its size. Most of the

balun configurations that can be found in the literature neglect this issue, but for some applications the output isolation is as important as the output amplitude and phase balance. Besides, for narrower bandwidths, the number of stages of the Wilkinson divider can be reduced. The prototype is implemented in microstrip technology on a Rogers 4350B substrate with relative permittivity of 3.66 and thickness of 30 mil at a design frequency $f_o = 3.5$ GHz.

The design of the pair of wire-bonded MTLs consists in finding out the number of strips k, the line-width W and spacing S in order to satisfy (12) and (13), equations that depend on both θ_d and Z_0. Therefore, by using [34] and the considerations given in [35], the achieved even and odd mode impedances for different W, S and $k = 4, 6$ are represented in Fig. 7. The theoretical values obtained by means of (12) and (13), considered as the design parameters and identified by circle, square and triangle marks, are also depicted for three impedance characteristics Z_0 (45, 50, 55) and five θ_d (90°, 80°, 70°, 60°, 50°). Hence, from this graph, once k, Z_0 and θ_d are chosen, the proper dimensions for the MTLs can be easily extracted. The shaded regions identify the allowed W and S values considering 100 μm as the limit dimension according to our fabrication capability. Design parameters for $k = 2$ or $k > 6$ are not represented because the required design impedances Z_{oe} and Z_{oo} for such number of conductors are very
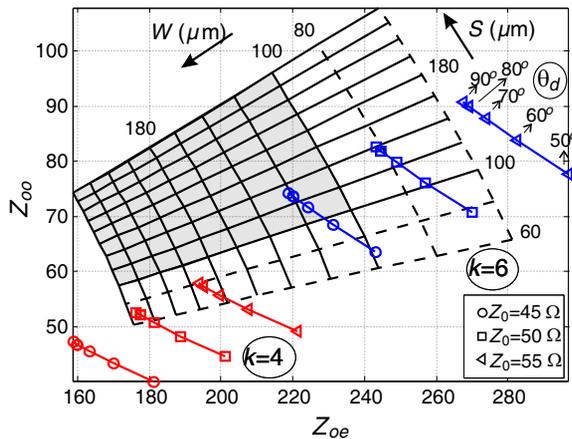
Figure 7. Achieved even and odd mode impedances as functions of the width W and spacing S between a pair of adjacent parallel transmission lines on the substrate RO4350B with $\epsilon_r = 3.66$ and thickness of 30 mil. The design values of impedances for $k = [4, 6]$, $\theta_d = [90, 80, 70, 60, 50]$ degrees and $Z_0 = [45, 50, 55]\,\Omega$ are also depicted. The design values are labeled with circle, square and triangle marks.

far from the obtained with the allowed W and S values ($> 100\,\mu$m). In addition, given Fig. 7, only if $k = 6$ and $Z_0 = 45\,\Omega$, values inside the shaded region are found. Besides, the minimum achievable value of θ_d is 63°, that is obtained with $W = 112\,\mu$m and $S = 100\,\mu$m. This value of θ_d determines a maximum attainable theoretical bandwidth of 110%, as shown in Fig. 6.

Furthermore, it may be interesting to analyze the behaviour of the phase shifting section to changes in W or S, or equivalently, in Z_{oe} and Z_{oo}. By inspection of Fig. 7, if the design curve for $k = 6$ and $Z_0 = 45\,\Omega$ is considered, it is easy to note that the curve is fully contained inside the range $W \in [100, 120]$ and $S \in [69, 137]$. Therefore, changing W or S respect to the computed nominal values for a particular design implies a modification on the characteristics of the shifting section, θ_d and Z_0. Besides, when a reference impedance that does not satisfy (13) is used, both amplitude and phase imbalance appear. The latter characteristic is exposed in Fig. 8 for two different designs, the first one with $Z_0 = 45\,\Omega$ and $\theta_d = 70°$, and the second one with $Z_0 = 45\,\Omega$ but $\theta_d = 90°$. In both cases, as shown, using a
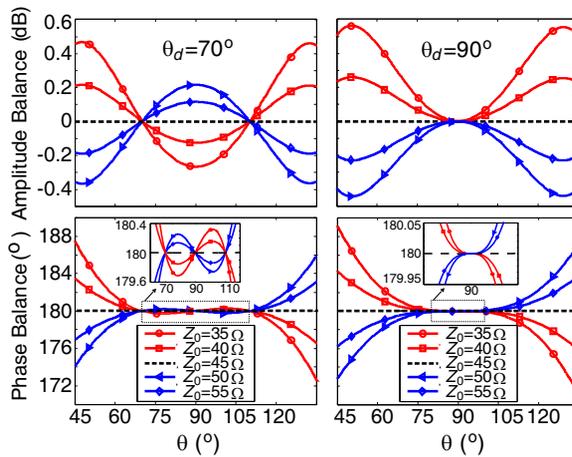

Figure 8. Amplitude and phase imbalance when a reference impedance different to the design impedance ($Z_0 = 45\,\Omega$) is used for two values of θ_d, 70° and 90°.

Table 2. Characteristics of the MTLs employed in the designed and fabricated balun at the center frequency $f_o = 3.5\,$GHz.

| θ_d (°)	k	W (µm)	S (µm)	ℓ (mm)
63	6	112	100	13.6

reference impedance different to the design one produce amplitude and
phase imbalance. As a result, variations in W and S or Z_0, modify
the frequency response of the two wire-bonded open-circuited and
short-circuited MTLs. Nevertheless, taking into account the results
of Fig. 8, small variations can be tolerated depending on the required
final performance.

Hence, by means of equations derived in Section 2.2 and Fig. 7,
one prototype of the proposed balun using the MTLs summarized in
Table 2 is fabricated and measured. A photograph of such a balun is
shown in Fig. 9, where the Wilkinson divider and the wire-bonded
short-circuited and open-circuited MTLs are clearly visible. The
measured return and insertion losses, isolation, and both amplitude
and phase balance are depicted in Fig. 10. Clearly it is observed
that good input matching and isolation are achieved. Insertion
losses and isolation are higher than 10 dB and 18 dB, respectively, in
the range [1–6] GHz (142%). Moreover, according to the amplitude
and phase balance, values remain lower than 0.4 dB and 5 degrees
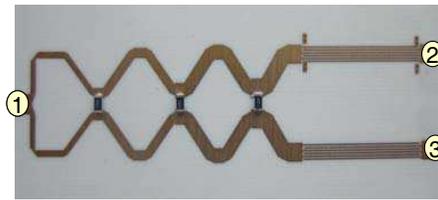
Figure 9. Photograph of the fabricated planar balun.
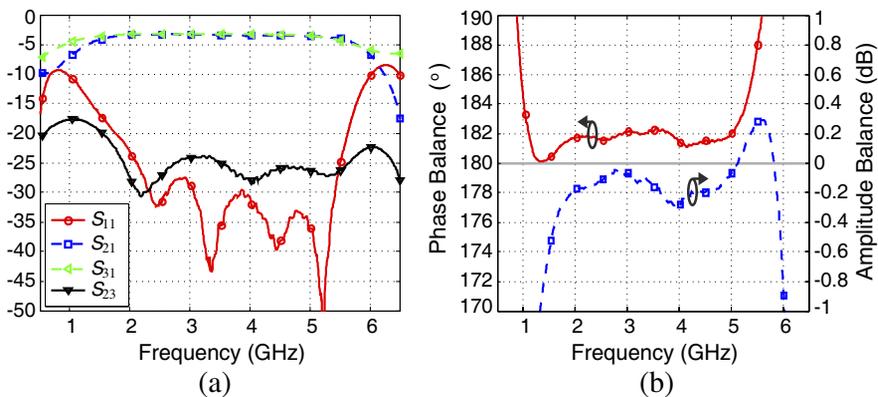
Figure 10. Measured scattering matrix elements and (a) amplitude
and (b) phase balance of the balun designed for $\theta_d = 63°$ (Table 2).

approximately, from 1.64 GHz up to 5.36 GHz, or equivalently over a fractional bandwidth of 106%. Therefore, by means of the general equations given in this work and considering values of θ_d different to the traditionally used 90 degrees, it is possible to design baluns with broader bandwidths.

As a way of integrating amplitude and phase offset into a single parameter, common-mode-rejection ratio (CMRR) is calculated. CMRR represents the splitter rejection of an undesired common-mode output signal resulting from a single-ended input signal. CMRR can be adapted as a measure of the imbalance in a 180 degrees splitter circuit, which can be determined from mixed-mode S-parameters or standard single-ended S-parameters as [36]

$$\text{CMRR} = \frac{S_{ds21}}{S_{cs21}} = \frac{S_{21} - S_{31}}{S_{21} + S_{31}}, \qquad (21)$$

where S_{ds21} and S_{cs21} identify the differential-mode and common-mode responses for a single-ended stimulus.

CMRR values, along with the S_{ds21} and S_{cs21} parameters, are displayed in Fig. 11 for the fabricated balun. CMRR can be used as a direct figure of merit to describe the quality of the balun and so interpreting the impact of amplitude and phase imbalances on the system performance. As seen, the designed balun provides high CMRR, greater than 30 dB within the frequency band [1.52–5.25] GHz. Furthermore, maximum CMRR values are located around the design θ_d, 2.2 GHz (θ_d) and 4.8 GHz ($180° - \theta_d$), approximately. Curves are not perfectly symmetrical respect to the center frequency 3.5 GHz due
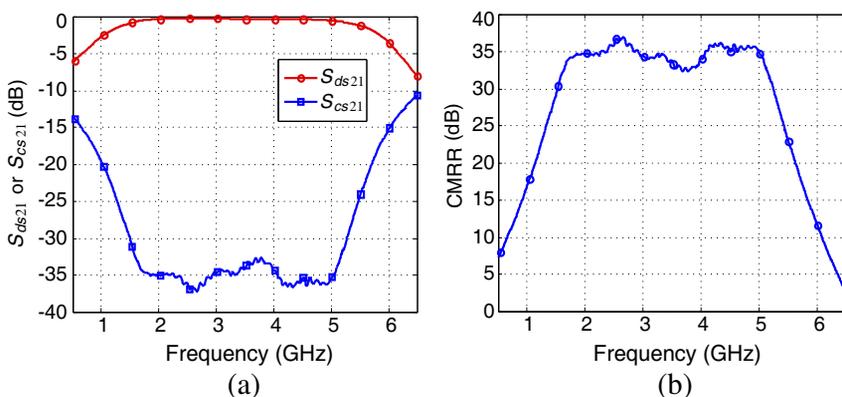
Figure 11. (a) Calculated S_{ds21}, S_{cs21} and (b) CMRR values using the measured S-parameters of the balun designed for $\theta_d = 63°$ (Table 2).

to the unequal even and odd mode phase velocities in the MTL, which difference increases with the frequency.

Finally, it should be highlighted that there has not been any optimization process during the electromagnetic simulations and all dimensions have been selected by following the design Equations (12) and (13). Besides, although results are good, it could be improved if the fabrication tolerances are overtaken because considerable variations of up to 10% have been measured.

4. CONCLUSION

A new theoretical study and design methodology of two open- and short-circuited wire-bonded MTLs has been presented when used for balance applications. Closed-form equations have been derived to properly design a 180° phase section and thus, a systematic procedure for the design of wire-bonded MTL baluns has been given. The analytical equations allow to calculate easily the dimensions of both MTLs to get a perfect output phase and amplitude balance at all frequencies, and perfect input matching at one or two frequencies as a function of the number of conductors. To assess the design guidelines, a microstrip planar balun has been designed, fabricated and measured. The balun presents measured amplitude and phase balance lower than $0.4\,\mathrm{dB}$ and 5 degrees over a 106% bandwidth, very close to the theoretical one of 110%. Furthermore, the presented balun has been proved to be an excelent alternative in order to obtain a perfect output isolation with values higher than $20\,\mathrm{dB}$.

Finally, it is worth to highlight that, according to the good measured results, the use of the analytical equations given in this work are advisable to obtain time-saving design procedures of other devices as filters, ring hybrids, rat-race couplers, DC blocks, coupled-line impedance transformer, and so on.

REFERENCES

1. Mongia, R., I. Bahl, and P. Bhartia, *RF and Microwave Coupled-Line Circuits*, Artech House, Norwood, MA, 1999.

2. Kumar, B. and G. Branner, "Optimized design of unique miniaturized planar baluns for wireless applications," *IEEE Microwave and Wireless Components Letters*, Vol. 13, No. 3, 134–136, Mar. 2003.

3. Ang, K. S., Y. Leong, and C. H. Lee, "Multisection impedance-transforming coupled-line baluns," *IEEE Transactions on Microwave Theory and Techniques*, Vol. 51, No. 2, 536–541, Feb. 2003.

4. Salah-Eddin, M. and A. Safwat, "Defected-ground coupled microstrip lines and its application in wideband baluns," *IET Microwaves, Antennas & Propagation*, Vol. 1, No. 4, 893–899, Aug. 2007.

5. Cloete, J., "Exact design of the marchand balun," *9th European Microwave Conference*, 480–484, Sep. 1979.

6. Nguyen, C. and D. Smith, "Novel miniaturised wideband baluns for MIC and MMIC applications," *Electronics Letters*, Vol. 29, No. 12, 1060–1061, Jun. 1993.

7. Tsai, M., "A new compact wideband balun," *IEEE Microwave and Millimeter-wave Monolithic Circuits Symposium*, 123–125, 1993.

8. Ang, K. S. and I. Robertson, "Analysis and design of impedance-transforming planar marchand baluns," *IEEE Transactions on Microwave Theory and Techniques*, Vol. 49, No. 2, 402–406, Feb. 2001.

9. Lu, J.-C., C.-C. Lin, and C.-Y. Chang, "Exact synthesis and implementation of new high-order wideband marchand baluns," *IEEE Transactions on Microwave Theory and Techniques*, Vol. 59, No. 1, 80–86, Jan. 2011.

10. Jacques, R. and D. Meignant, "Novel wide band microstrip balun," *11th European Microwave Conference*, 839–843, Sep. 1981.

11. Rogers, J. and R. Bhatia, "A 6 to 20 GHz planar balun using a wilkinson divider and lange couplers," *IEEE MTT-S International Microwave Symposium Digest*, Vol. 2, 865–868, Jul. 1991.

12. Zhang, Z.-Y., Y.-X. Guo, L. C. Ong, and M. Chia, "A new wide-band planar balun on a single-layer PCB," *IEEE Microwave and Wireless Components Letters*, Vol. 15, No. 6, 416–418, Jun. 2005.

13. Antoniades, M. and G. Eleftheriades, "A broadband Wilkinson balun using microstrip metamaterial lines," *IEEE Antennas and Wireless Propagation Letters*, Vol. 4, 209–212, 2005.

14. Tseng, C.-H. and C.-L. Chang, "Wide-band balun using composite right/left-handed transmission line," *Electronics Letters*, Vol. 43, No. 21, 1154–1155, Nov. 2007.

15. Chongcheawchamnan, M., C. Y. Ng, K. Bandudej, A. Worapishet, and I. Robertson, "On miniaturization isolation network of an all-ports matched impedance-transforming marchand balun," *IEEE Microwave and Wireless Components Letters*, Vol. 13, No. 7, 281–283, Jul. 2003.

16. Cobos-Bandera, S., J. J. Sánchez-Martínez, and E. Márquez-Segura, "Mems-based reconfigurable test-set for differential and common mode measurement using a two-port network analyzer," *42nd European Microwave Conference (EuMC)*, Oct. 2012.

17. Faria, J. A. B., *Multiconductor Transmission-line Structures: Modal Analysis Techniques*, Wiley, New York, 1993.

18. Paul, C. R., *Analysis of Multiconductor Transmission Line*, Wiley, New York, 1994.

19. Márquez-Segura, E., F. Casares-Miranda, P. Otero, C. Camacho-Peñalosa, and J. Page, "Analytical model of the wire-bonded interdigital capacitor," *IEEE Transactions on Microwave Theory and Techniques*, Vol. 54, No. 2, 748–754, Feb. 2006.

20. Casares-Miranda, F., P. Otero, E. Márquez-Segura, and C. Camacho-Peñalosa, "Wire bonded interdigital capacitor," *IEEE Microwave and Wireless Components Letters*, Vol. 15, No. 10, 700–702, Oct. 2005.

21. March, S., "A wideband stripline hybrid ring (correspondence)," *IEEE Transactions on Microwave Theory and Techniques*, Vol. 16, No. 6, 361, Jun. 1968.

22. Sánchez-Martínez, J. J., E. Márquez-Segura, P. Otero, and C. Camacho-Peñalosa, "Artificial transmission line with left/right-handed behavior based on wire bonded interdigital capacitors," *Progress In Electromagnetics Research B*, Vol. 11, 245–264, 2009.

23. Sánchez-Martínez, J. J., E. Márquez-Segura, and C. Camacho-Peñalosa, "Synthesis of CRLH-TLs based on a shunt coupled-line section," *42nd European Microwave Conference (EuMC)*, 2012.

24. Liu, G.-Q., L.-S. Wu, and W.-Y. Yin, "A compact microstrip rat-race coupler with modified lange and t-shaped arms," *Progress In Electromagnetics Research*, Vol. 115, 509–523, 2011.

25. Sánchez-Martínez, J. J. and E. Márquez-Segura, "Analytical study of wide-band bandpass filters based on wire-bonded multiconductor transmission lines with LH behaviour," *Progress In Electromagnetics Research Letters*, Vol. 31, 1–13, 2012.

26. Kuo, J.-T., C.-Y. Fan, and S.-C. Tang, "Dual-wideband bandpass filters with extended stopband based on coupled-line and coupled three-line resonators," *Progress In Electromagnetics Research*,

Vol. 124, 1–15, 2012.

27. Li, S., B. Tang, Y. Liu, S. Li, C. Yu, and Y. Wu, "Miniaturized dual-band matching technique based on coupled-line transformer for dual-band power amplifiers design," *Progress In Electromagnetics Research*, Vol. 131, 195–210, 2012.

28. Li, B., X. Wu, N. Yang, and W. Wu, "Dual-band equal/unequal Wilkinson power dividers based on coupled-line section with short-circuited stub," *Progress In Electromagnetics Research*, Vol. 111, 163–178, 2011.

29. Ou, W., "Design equations for an interdigitated directional coupler," *IEEE Transactions on Microwave Theory and Techniques*, Vol. 23, No. 2, 253–255, Feb. 1975.

30. Kajfez, D. and B. Vidula, "Design equations for symmetric microstrip dc blocks," *IEEE Transactions on Microwave Theory and Techniques*, Vol. 28, No. 9, 974–981, Sep. 1980.

31. Page, J., E. Márquez-Segura, F. Casares-Miranda, J. Esteban, P. Otero, and C. Camacho-Peñalosa, "Exact analysis of the wire-bonded multiconductor transmission line," *IEEE Transactions on Microwave Theory and Techniques*, Vol. 55, No. 8, 1585–1592, Aug. 2007.

32. Pozar, D., *Microwave Engineering*, 2nd Edition, Wiley, New York, 1998.

33. Cohn, S., "A class of broadband three-port TEM-mode hybrids," *IEEE Transactions on Microwave Theory and Techniques*, Vol. 19, No. 2, 110–116, Feb. 1968.

34. Kirschning, M. and R. Jansen, "Accurate wide-range design equations for the frequency-dependent characteristic of parallel coupled microstrip lines," *IEEE Transactions on Microwave Theory and Techniques*, Vol. 32, No. 1, 83–90, Jan. 1984.

35. Faria, J. A. B., "Kirschning and Jansen computer-aided design formulae for the analysis of parallel coupled lines," *Microwave and Optical Technology Letters*, Vol. 51, No. 10, 2466–2470, 2009.

36. Eisenstadt, W. R., B. Stengel, and B. M. Thompson, *Microwave Differential Circuit Design Using Mixed-mode S-parameters*, Artech House, Norwood, MA, 2006.